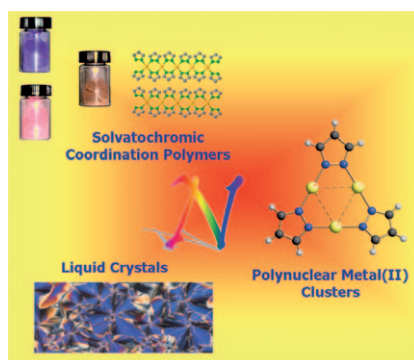


Versatile ligands: Very minor changes in connectivity, composition, and polarity of the molecular entities employed in self-assembly reactions significantly affect the structural, thermal, sorptive, magnetic, and mesomorphic behavior of the resulting materials (see scheme).



Coordination Polymers

C. Pettinari,* N. Masciocchi,
L. Pandolfo, D. Pucci 1106–1123

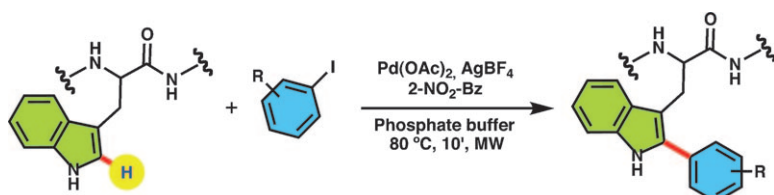
Tuning the Functional Properties of Metal Complexes Containing Polytopic Heteroaromatic Nitrogen Ligands

COMMUNICATIONS

Peptide Modifications

J. Ruiz-Rodríguez, F. Albericio,*
R. Lavilla* 1124–1127

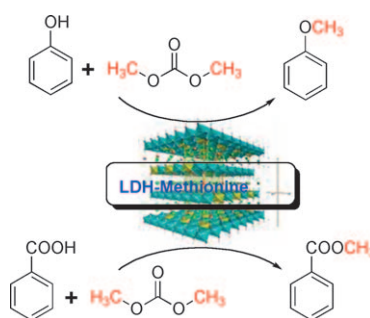
Postsynthetic Modification of Peptides: Chemoselective C-Arylation of Tryptophan Residues



Born to be mild: The general, direct and selective C2 arylation of native Trp-containing peptides can be achieved by palladium-catalyzed C–H activation with aryl iodides in water,

under microwave irradiation for a short time (see scheme). Under these mild conditions, the structural and stereochemical integrity of peptides is preserved.

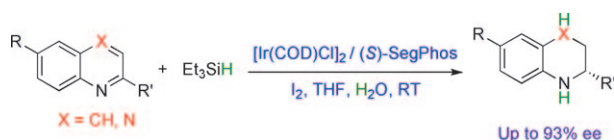
Simple methodology: A layered double hydroxide-supported L-methionine (LDH-Met) catalyst is designed in a simple methodology to explore its synthetic utility in biologically relevant reactions. The organocatalyst is characterized by FT-IR, TGA/DTA, powder XRD, and EDX spectroscopic techniques. This material has been successfully utilized for the preparation of aryl methyl ethers and esters from the corresponding phenols and carboxylic acids, respectively, in moderate to high yields (see scheme).



Heterogeneous Catalysis

A. Dhakshinamoorthy, A. Sharmila,
K. Pitchumani* 1128–1132

Layered Double Hydroxide-Supported L-Methionine-Catalyzed Chemoselective O-Methylation of Phenols and Esterification of Carboxylic Acids with Dimethyl Carbonate: A “Green” Protocol



Water as a hydride source: A new pathway to form metal–hydride bonds has been developed through the reaction of easily available metal–silyl compounds with water. This method

has been successfully applied to asymmetric hydrogenation of heteroaromatic compounds with up to 93 % ee under mild autoclave-free conditions (see scheme).


Metal–Hydride Bonds

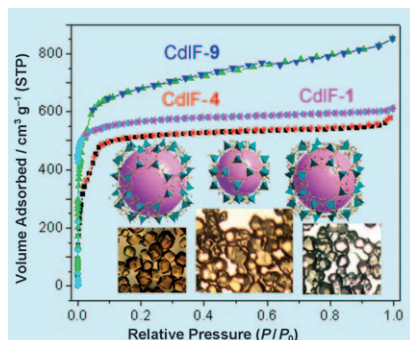
D.-W. Wang, D.-S. Wang, Q.-A. Chen,
Y.-G. Zhou* 1133–1136

Asymmetric Hydrogenation with Water/Silane as the Hydrogen Source

Metal–Organic Frameworks

Y.-Q. Tian,* S.-Y. Yao, D. Gu,
K.-H. Cui, D.-W. Guo, G. Zhang,
Z.-X. Chen, D.-Y. Zhao*... 1137–1141


 **Cadmium Imidazolate Frameworks with Polymorphism, High Thermal Stability, and a Large Surface Area**

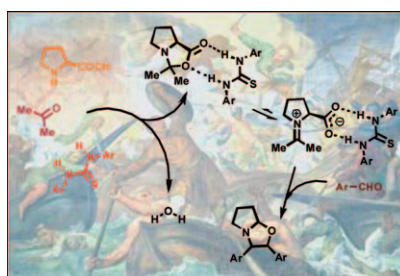


Polymorphous cadmium 2-substituent imidazolate frameworks (CdIFs) with high porosity and thermal stability have been realized (see figure). The use of cadmium results in the elongation of M–N bonds and increased flexibility of the M–N bond rotation resulting in polymorphism, high porosity, and thermal stability.

Organocatalysis

N. El-Hamdouni, X. Companyó,
R. Rios,* A. Moyano*... 1142–1148


 **Substrate-Dependent Nonlinear Effects in Proline–Thiourea-Catalyzed Aldol Reactions: Unraveling the Role of the Thiourea Co-Catalyst**

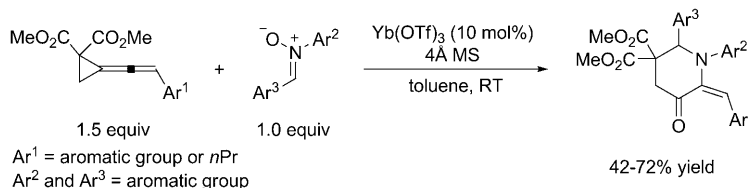


It's an affair of four: The study of non-linear effects in the proline–thiourea-catalyzed aldol reaction between acetone and aromatic aldehydes, together with NMR and ESI-MS experiments, shows that the main role of the thiourea co-catalyst is that of promoting both the formation of a soluble Seebach's oxazolidinone intermediate and its conversion into the iminium carboxylate isomer.

Indole Chemistry

L. Wu, D. M. Shi*... 1149–1152

 **Yb(OTf)₃-Catalyzed Construction of Indole Derivatives through Formal [3+3] Cycloaddition of 1,1-Vinylidene-cyclopropanediester with Nitrones**




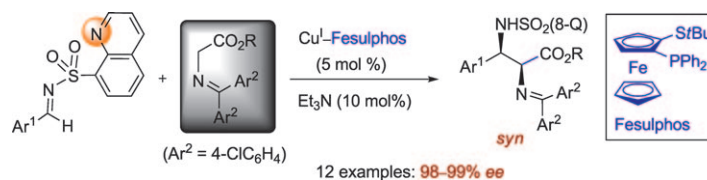
Indulging in indoles: Indole derivatives are efficiently afforded through Yb(OTf)₃-catalyzed formal [3+3] cycloaddition of 1,1-vinylidene-cyclopro-

panediester with nitrones in moderate to good yields under mild reaction conditions (see scheme).

Mannich Reaction

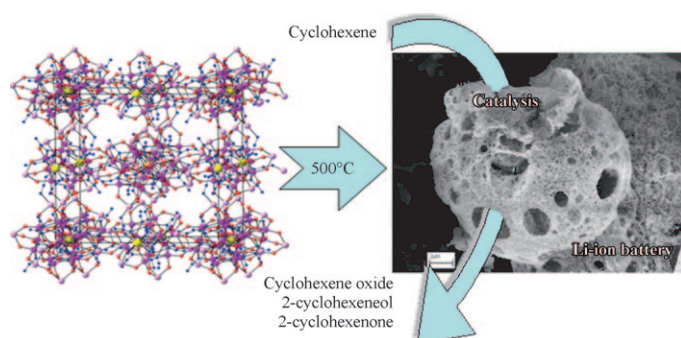
J. Hernández-Toribio,
R. Gómez Arrayás,*
J. C. Carretero*... 1153–1157

 **Substrate-Controlled Diastereoselectivity Switch in Catalytic Asymmetric Direct Mannich Reaction of Glycine Derivatives with Imines: From *anti*- to *syn*- α,β -Diamino Acids**



Back and forth: A diastereoselectivity switch has been devised in the Fesulphos–Cu^I-catalyzed glycine direct Mannich reaction with *N*-(8-quinolyl)sulfonyl imines by tuning the steric and electronic properties of the glycine component (see scheme). α,β -Diamino

acids of *syn* configuration are produced under high diastereo- and enantiocontrol with glycinate esters derived from electron-deficient benzophenone-type ketimines, in contrast to aldimine-derived pronucleophiles that lead to *anti*-configured products.



Pores for thought! Thermolysis of a 3D coordination network of $\text{Mn}^{\text{II}}/\text{Mn}^{\text{III}}$ produces a novel spongelike morphology of manganese oxide by a degassing mechanism (see picture). This porous

material shows high capacitance when used as an anode in a Li-ion battery and efficient catalytic activity for cyclohexene oxidation.

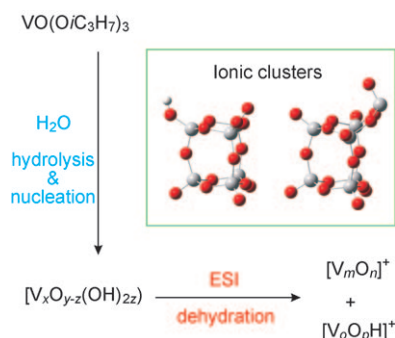
Porous Materials

S. Nayak, S. Malik, S. Indris, J. Reedijk, A. K. Powell* 1158–1162

Pyrolysis of a Three-Dimensional $\text{Mn}^{\text{II}}/\text{Mn}^{\text{III}}$ Network To Give a Multi-functional Porous Manganese Oxide Material



H_2O , then no H_2O : A new protocol combining sol-gel processing with electrospray ionization can produce charged metal oxide clusters from the mononuclear precursor $\text{VO}(\text{O}i\text{C}_3\text{H}_7)_3$. The size range of vanadium oxide cluster ions in the gas phase was extended significantly up to $[\text{V}_{30}\text{O}_{75}\text{H}]^+$ (m/z 2728).



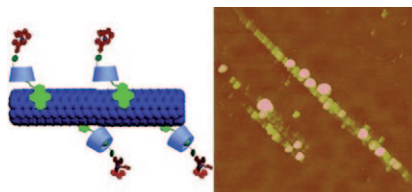
Metal Oxide Clusters

X. Zhang, H. Schwarz* 1163–1167

Generation of Gas-Phase Nanosized Vanadium Oxide Clusters from a Mononuclear Precursor by Solution Nucleation and Electrospray Ionization



Take control! A supramolecular hybrid has been prepared by the non-covalent surface modification of single-walled carbon nanotubes (SWCNT) with cationic β -cyclodextrin-tethered ruthenium complexes through a spacer (see figure). The cationic ruthenium-complex-decorated SWCNTs spatially control DNA condensation and can be used as a potential nonviral gene delivery system.



FULL PAPERS

Supramolecular Structures


M. Yu, S.-Z. Zu, Y. Chen, Y.-P. Liu, B.-H. Han,* Y. Liu* 1168–1174

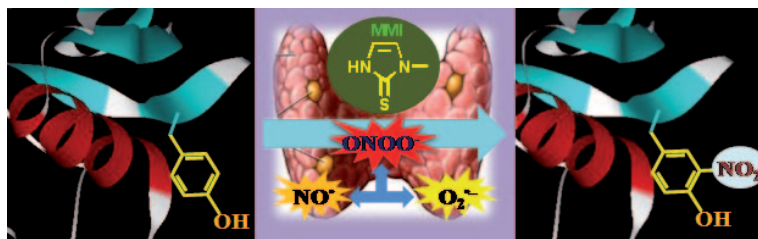
Spatially Controllable DNA Condensation by a Water-Soluble Supramolecular Hybrid of Single-Walled Carbon Nanotubes and β -Cyclodextrin-Tethered Ruthenium Complexes



Protein Nitration

K. P. Bhabak, G. Mugesh* . . 1175–1185

 **Antithyroid Drugs and their Analogues Protect Against Peroxynitrite-Mediated Protein Tyrosine Nitration—A Mechanistic Study**




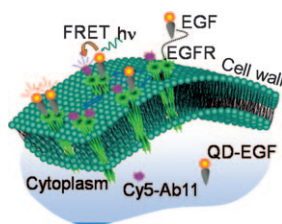
Way out west: The effect of some commonly used antithyroid drugs and their analogues on peroxynitrite-mediated nitration of proteins is described. The nitration was studied by Western blot analysis. These studies reveal that the

antithyroid drugs MMI, PTU, MTU and their analogues with thione and selone moieties significantly reduce the tyrosine nitration of both BSA and cytochrome c.

Single Molecules

N. Kawashima, K. Nakayama, K. Itoh, T. Itoh, M. Ishikawa, V. Biju* 1186–1192

 **Reversible Dimerization of EGFR Revealed by Single-Molecule Fluorescence Imaging Using Quantum Dots**

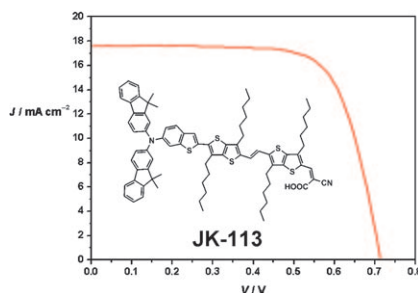


Receptors hug repeatedly: Intermolecular interactions among receptors and ligands are essential for cell-signaling and regular growth and functioning of cells. Single-molecule fluorescence imaging and spectroscopy of EGFR in cells have shown that reversible dimerization among heterodimers and pre-dimers is essential for the lateral propagation of cell signaling and continuous generation of signaling molecules.

Dye-Sensitized Solar Cells

H. Choi, I. Raabe, D. Kim, F. Teocoli, C. Kim, K. Song, J.-H. Yum, J. Ko,* Md. K. Nazeeruddin,* M. Grätzel* 1193–1201


High Molar Extinction Coefficient Organic Sensitizers for Efficient Dye-Sensitized Solar Cells

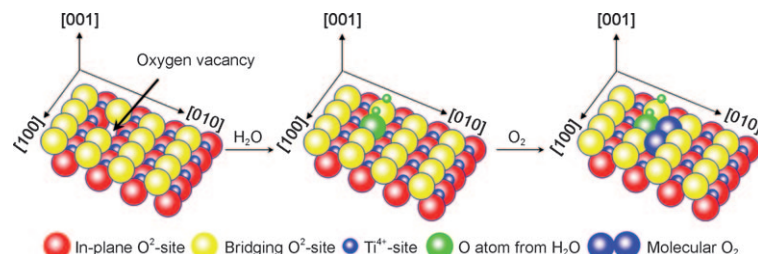


On the rise! We have designed and synthesized highly efficient organic sensitizers with a planar thienothiophene–vinylene–thienothiophene linker. Solar-cell devices based on the sensitizer **JK-113** (see picture) in conjunction with a volatile electrolyte and a solvent-free ionic liquid electrolyte gave high conversion efficiencies of 9.1 % and 7.9 %, respectively. The **JK-113**-based solar cell fabricated by using a solvent-free ionic liquid electrolyte showed excellent stability under light soaking at 60 °C for 1000 h.

Surface Chemistry

Z. Zheng, J. Teo, X. Chen, H. Liu, Y. Yuan, E. R. Waclawik, Z. Zhong,* H. Zhu* 1202–1211

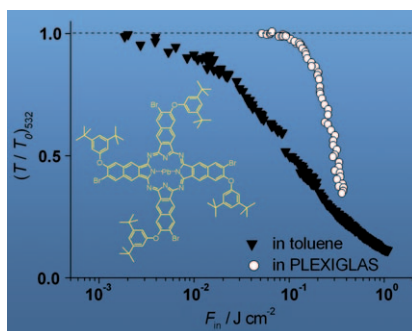
 **Correlation of the Catalytic Activity for Oxidation Taking Place on Various TiO₂ Surfaces with Surface OH Groups and Surface Oxygen Vacancies**



Catalytic oxidation: Surface rehydroxylation ability is an indicator of TiO₂-based catalysts for catalytic and photocatalytic oxidations with molecular O₂ as the oxidant, because it indicates the

concentration of surface oxygen vacancies, which result in H₂O and O₂ adsorption on the TiO₂ surface and supply active O₂ for the oxidation reactions (see figure).

A Pb naphthalocyanine for optical limiting: Naphthalocyanines limit the power of intense radiations through optical self-activation. Brominated lead naphthalocyanine (see figure) in Plexiglas displays reversible optical limiting of ns pulses within the Vis/NIR range.



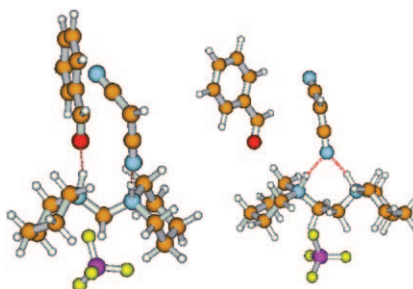
Optical Power Limiting

D. Dini, M. Meneghetti,*
M. J. F. Calvete, T. Arndt, C. Liddiard,
M. Hanack* 1212–1220

Tetrabrominated Lead Naphthalocyanine for Optical Power Limiting



Strong distance relationship: The enhanced activity of bifunctional acid–base ionic liquid organocatalysts is due to a cooperative effect between the acidic and basic centres that—as has been found to be the case with enzymes—is determined by the distance between the two sites (see figure).

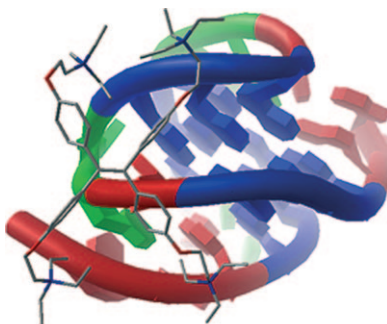


Ionic Liquids

M. Boronat, M. J. Climent, A. Corma,
S. Iborra, R. Montón,
M. J. Sabater* 1221–1231

Bifunctional Acid–Base Ionic Liquid Organocatalysts with a Controlled Distance Between Acid and Base Sites

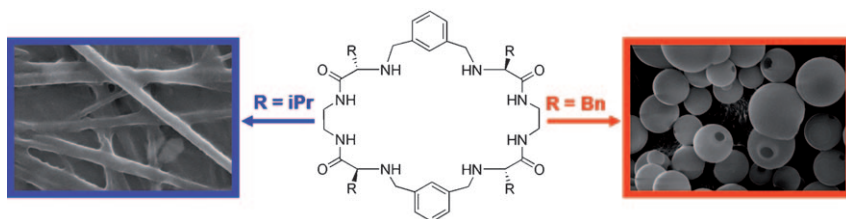
Specific binding: A water-soluble fluorogen shows a strong emission towards a specific G-quadruplex structure formed by a human telomeric sequence, but not other DNA conformers, due to the preferred structural matching in the docking process of the fluorogen on the G-quadruplex surface (see figure) with the aid of electrostatic attraction.



Biosensors

*Y. Hong, H. Xiong, J. W. Y. Lam,
M. Häußler, J. Liu, Y. Yu, Y. Zhong,
H. H. Y. Sung, I. D. Williams,
K. S. Wong, B. Z. Tang** 1232–1245

Fluorescent Bioprobes: Structural Matching in the Docking Processes of Aggregation-Induced Emission Fluorogens on DNA Surfaces



Straight or round? Studies using electronic microscopy, ^1H NMR, UV/CD, and FTIR spectroscopy show that intermolecular hydrogen-bonding and π – π interactions determine the self-assembly of pseudo-peptidic macrocy-

cles into a variety of structures. The nature of the amino acid side chain can determine the morphology of the obtained nanostructure from long fibers to hollow spheres (see picture).

Nanostructures

I. Alfonso, M. Bru, M. I. Burguete,
E. García-Verdugo,
S. V. Luis** 1246–1255

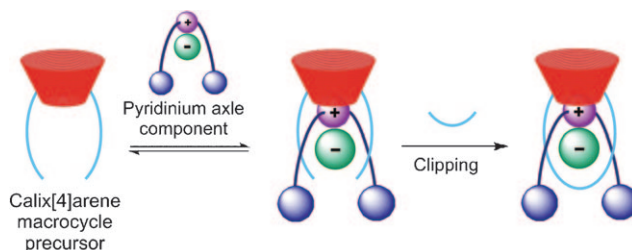
Structural Diversity in the Self-Assembly of Pseudo-peptidic Macrocycles



Anion Recognition

A. J. McConnell, C. J. Serpell,
A. L. Thompson, D. R. Allan,
P. D. Beer* 1256–1264

Calix[4]arene-Based Rotaxane Host Systems for Anion Recognition



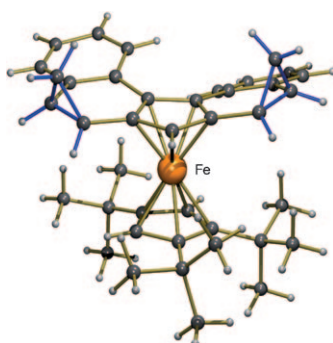
Spokes in a wheel: The synthesis, structure and anion-binding properties of the first calix[4]arene-based [2]rotaxane anion host systems are described (see figure). Anion-binding

studies reveal that preorganisation of the interlocked host cavity determines the strength and selectivity of anion binding in protic media.

Aromaticity

F. Pammer, Y. Sun, D. Weismann,
H. Sitzmann, W. R. Thiel* . . 1265–1270

Exploring the Concept of Aromaticity on Complexes of a Fourfold Benzanulated Cyclopentadienyl Ligand

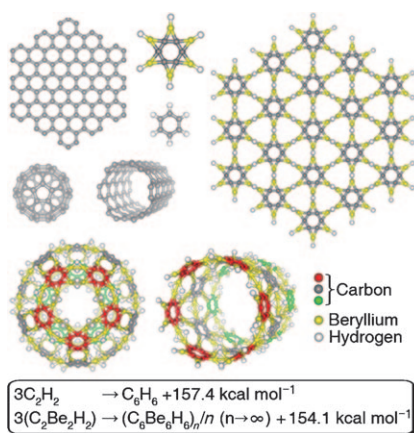


Enhanced localization of aromaticity in the terminal rings and in the central five-membered ring of dibenzo-[c,g]fluorene gives rise to a typical C=C double bond type of reactivity at two distinct positions of the ligand. This was evaluated theoretically and by cyclopropanation (see example in structure shown).

Nanostructures

Y.-B. Wu, J.-L. Jiang, R.-W. Zhang,
Z.-X. Wang* 1271–1280

Computationally Designed Families of Flat, Tubular, and Cage Molecules Assembled with “Starbenzene” Building Blocks through Hydrogen-Bridge Bonds

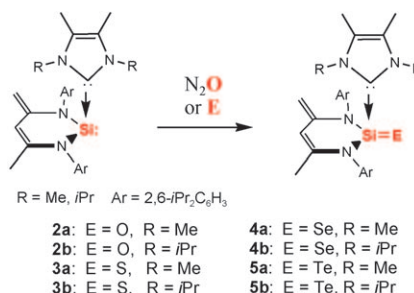


Starring role: Graphenes, carbon nanotubes, and fullerenes use classical sp²-hybridized carbon atoms as basic units. Now, DFT calculations indicate that the unconventional planar tetra-coordinated carbon could also be used to construct such shaped molecules, but with different chemical bonding (see depicted examples). They were predicted to have reasonable stabilities, which imply that they could be realized experimentally for potential applications.

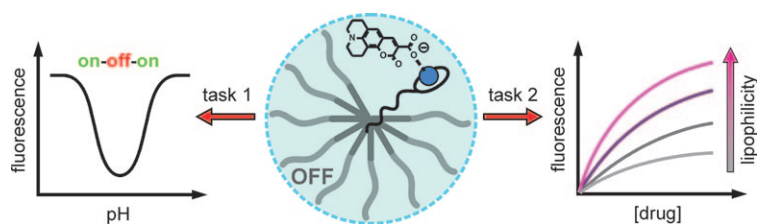
Chalcogens

S. Yao, Y. Xiong,
M. Driess* 1281–1288

N-Heterocyclic Carbene (NHC)-Stabilized Silanechalcogenones: NHC→Si(R)₂=E (E = O, S, Se, Te)



Stable silicon series: The first entire series of N-heterocyclic carbene stabilized silanechalcogenones **2a,b** (Si=O), **3a,b** (Si=S), **4a,b** (Si=Se), and **5a,b** (Si=Te) is reported (see graphic). These were prepared by gentle oxidation of the carbene-silylene adducts with N₂O (in the case of **2a,b**) and elemental chalcogens.



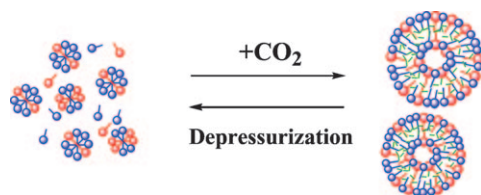
A gauge and a window: A self-assembled micellar device is capable of carrying out two different and tricky sensing activities: it signals pH windows with the rare well-like (“on–off–on”)

fluorescent response, and is capable of measuring the lipophilicity of molecules at the physiological pH value of 7.4 by means of an easy-to-read fluorescence-reviving signal (see graphic).

Molecular Sensors

F. Denat, Y. A. Diaz-Fernandez, L. Pasotti, N. Sok, P. Pallavicini* 1289–1295

A Micellar Multitasking Device: Sensing pH Windows and Gauging the Lipophilicity of Drugs with Fluorescent Signals



Making the transition: Compressed CO₂ induces the micelle-to-vesicle transition (MVT) in a dodecyltrimethylammonium bromide (DTAB)/sodium dodecyl sulfate (SDS) mixed aqueous surfactant system. The vesicles reform micelles simply by depressurization.

Therefore, CO₂ can be used to switch the MVT reversibly by controlling pressure (see scheme). The mechanism behind the use of gas to induce the MVT is different from the use of polar and electrolyte additives.

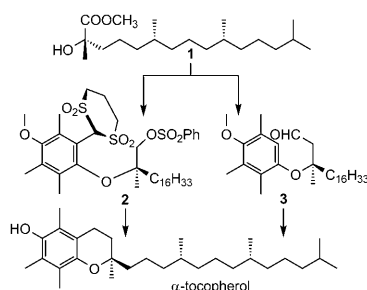
Mixed Surfactant Systems

W. Li, J. Zhang, Y. Zhao, M. Hou, B. Han,* C. Yu, J. Ye 1296–1305

Reversible Switching of a Micelle-to-Vesicle Transition by Compressed CO₂



Complete inversion: Mitsunobu reaction of the chiral α -hydroxy ester **1** with suitably substituted hydroquinones gave under complete inversion of configuration the sulfone **2**, and after C₁ homologation the aldehyde **3** (see scheme). Both intermediates were cyclized to the chromanol system of α -tocopherol, obtained in 94% diastereomeric excess.

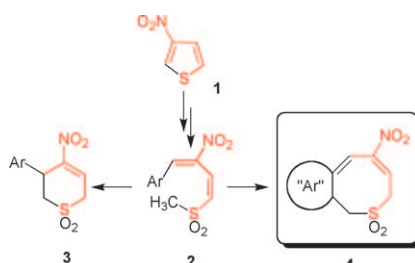


Vitamin E Family

U. Hengartner, A. Choungnet, K. Liu, W.-D. Woggon* 1306–1311

Asymmetric Synthesis of α -Tocopherol

Playing with sulfur heterocycles: The interesting fused-ring derivatives **4**, characterized by an unusual eight-membered sulfur heterocycle, have been found to significantly enrich the pool of heterocycles obtainable through overall ring expansion from 3-nitrothiophene (**1**). Rationalization is provided for the formation of **4** in competition with the isomeric thio-pyrans **3**.



Nitrothiophenes

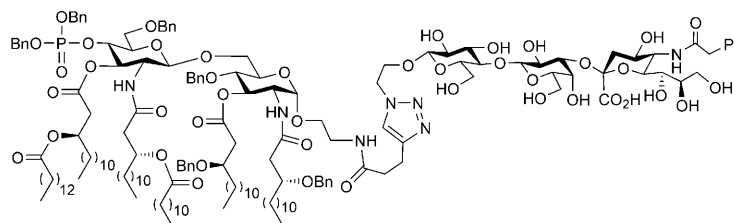
L. Bianchi, G. Giorgi, M. Maccagno, G. Petrillo, F. Sancassan, E. Severi, D. Spinelli, M. Stenta, C. Tavani* 1312–1318

Ring-Opening/Ring-Closing Protocols from Nitrothiophenes: Six-Membered versus Unusual Eight-Membered Sulfur Heterocycles through Michael-Type Addition on Nitrobutadienes

Glycolipid Derivatives

S. Tang, Q. Wang, Z. Guo* 1319–1325

Synthesis of a Monophosphoryl Derivative of *Escherichia coli* Lipid A and Its Efficient Coupling to a Tumor-Associated Carbohydrate Antigen



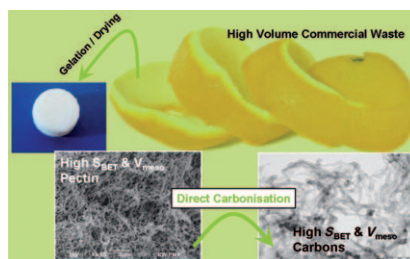
Synthesis of monophosphoryl lipid A conjugate: A convergent and efficient synthesis of a monophosphoryl derivative of *E. coli* lipid A is described (see graphic), which is suitable for coupling

with various molecules, as well as with tumor-associated antigens for the development of carbohydrate-based cancer vaccines.

Mesoporous Materials

R. J. White,* V. L. Budarin,
J. H. Clark 1326–1335

Pectin-Derived Porous Materials

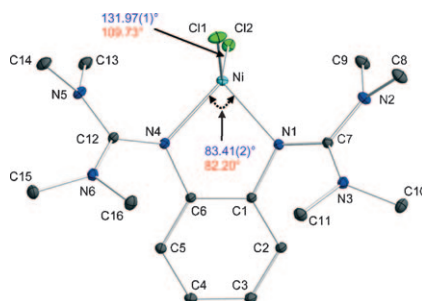


Ap“peel”ingly simple! The simple sustainable preparation of highly porous pectins ($S_{\text{BET}} > 200 \text{ m}^2 \text{ g}^{-1}$) as powders or monoliths is presented. Direct carbonisation of these “green” precursors yields highly mesoporous ($V_{\text{meso}} > 0.4 \text{ cm}^3 \text{ g}^{-1}$) low-density carbonaceous materials (see picture). The pectin gelation route allows direction of nanoscale morphology, whilst carbonisation temperature provides control over surface chemistry. Importantly highly mesoporous functionally rich carbonaceous materials are prepared without template or catalyst.

Coordination Compounds

P. Roquette, A. Maronna, A. Peters,
E. Kaifer, H.-J. Himmel,* C. Hauf,
V. Herz, E.-W. Scheidt,
W. Scherer* 1336–1350

On the Electronic Structure of Ni^{II} Complexes That Feature Chelating Bisguanidine Ligands

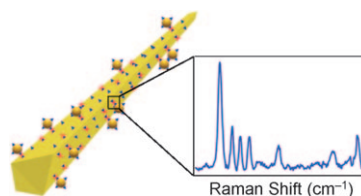


Extremely basic but innocent: Super-basic bisguanidines were used as ligands in new Ni complexes (e.g., $[(\text{btmgb})\text{NiCl}_2]$; btmgb = bis(tetramethylguanidino)benzene; see ORTEP plot). The structural and electronic properties (including the paramagnetism) of these complexes have been analyzed.

Nanomaterials

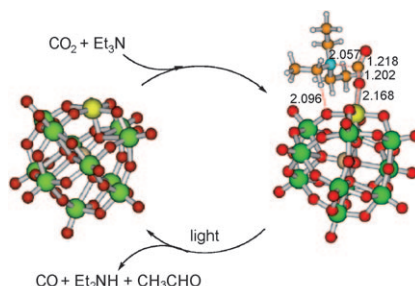
T. Kang, I. Yoon, J. Kim, H. Ihee,
B. Kim* 1351–1355

Au Nanowire–Au Nanoparticles Conjugated System which Provides Micrometer Size Molecular Sensors



Nano gold: We report a new surface-enhanced Raman scattering (SERS) sensor for biomolecule detection through a Au nanowire (NW)–Au nanoparticles (NPs) conjugated system. Biotinylated NPs are self-assembled on the NW through avidin; this creates hot spots between NW and NPs. The label-free avidin can be detected with high sensitivity and selectivity.

Reduced circumstances: A polyoxometalate of the Keggin structure substituted with Ru^{III} catalyzes the photoreduction of CO₂ to CO with tertiary amines as reducing agents (see picture). UV/Vis, EPR, and ¹³C NMR spectroscopy enabled determination of the coordination of CO₂ to the ruthenium center of the polyoxometalate. DFT calculations showed the preferred binding mode of CO₂ to the polyoxometalate and the electronic structure of bound CO₂.



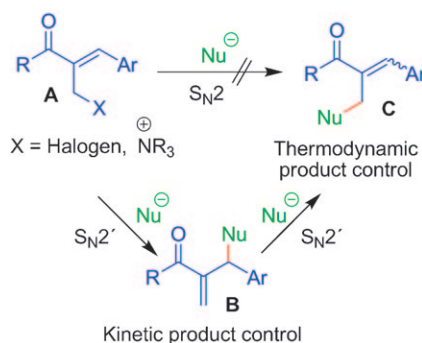
Polyoxometalates

A. M. Khenkin, I. Efremenko,
L. Weiner, J. M. L. Martin,
R. Neumann* 1356–1364

Photochemical Reduction of Carbon Dioxide Catalyzed by a Ruthenium-Substituted Polyoxometalate



S_N2' beats S_N2: Baylis–Hillman adducts **A**, in which X is a good leaving group, react with stabilized carbanions to give the S_N2' products **B** selectively. When the carbanions are used in excess, a second S_N2' reaction yields the thermodynamically favored isomers **C**. From the kinetics of the reactions of the allylammonium ions **A** (X = ⁺NR₃) with carbanions, electrophilicity parameters *E* for the electrophiles **A** (X = ⁺NR₃) have been derived.



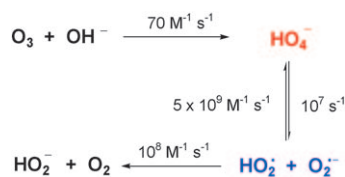
Controlling Regioselectivity

M. Baidya, G. Y. Remennikov,
P. Mayer, H. Mayr* 1365–1371

S_N2' versus S_N2 Reactivity: Control of Regioselectivity in Conversions of Baylis–Hillman Adducts



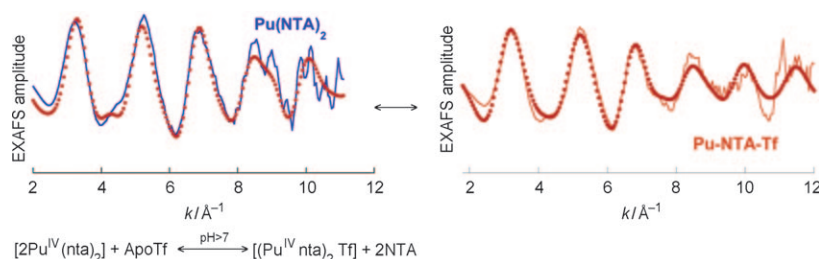
Super oxides: Ozone reacts with OH[−] to form HO₄[−], which is in equilibrium with HO₂[•] and O₂^{•−}. These only decay slowly into HO₂[−] and O₂ (see scheme). Because of the importance of HO₂[•]/O₂^{•−} in our biosphere, HO₄[−] must be one of the most abundant short-lived nonradical intermediates.



Reaction Mechanisms

G. Merényi,* J. Lind, S. Naumov,
C. von Sonntag* 1372–1377

The Reaction of Ozone with the Hydroxide Ion: Mechanistic Considerations Based on Thermokinetic and Quantum Chemical Calculations and the Role of HO₄[−] in Superoxide Dismutation



A protein binds actinides: Transferrin (Tf), the iron-transport protein in the serum, has been shown to take up neptunium and plutonium at oxidation state +IV. A molecular description of

the actinide binding site has been proposed on the basis of several techniques, among them EXAFS (see figure).

Actinide Binding

A. Jeanson, M. Ferrand, H. Funke,
C. Hennig, P. Moisy, P. L. Solari,
C. Vidaud, C. Den Auwer* .. 1378–1387

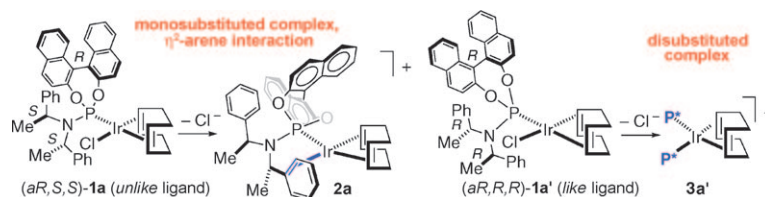
The Role of Transferrin in Actinide(IV) Uptake: Comparison with Iron(III)

Phosphoramidite Ligands

T. Osswald, H. Rüegger,
A. Mezzetti* 1388–1397



Secondary Interactions or Ligand Scrambling? Subtle Steric Effects Govern the Iridium(I) Coordination Chemistry of Phosphoramidite Ligands



Like or unlike? Depending on the relative configuration of the binaphthol and benzyl groups, chloride abstraction (see picture) gives either the chelate complex **2a** (*unlike* P*) or the disubstituted species **3a'** (*like* P*). This obser-

vation may explain the apparently random stereochemical results obtained in asymmetric catalysis with diastereoisomeric phosphoramidite ligands.

* Author to whom correspondence should be addressed



Supporting information on the WWW (see article for access details).



Full Papers labeled with this symbol have been judged by two referees as being “very important papers”.



A video clip is available as Supporting Information on the WWW (see article for access details).

SERVICE

Spotlights 1102 Author Index 1398 Keyword Index 1399 Preview 1401

Issue 3/2010 was published online on January 14, 2010

CORRIGENDUM

T. Haino,* K. Fukuta, H. Iwamoto,
S. Iwata* 13286–13290

Noncovalent Isotope Effect for Guest Encapsulation in Self-Assembled Molecular Capsules

Chem. Eur. J., **2009**, *15*

DOI: 10.1002/chem.200902526

References [1] and [16] of this Communication appeared incorrectly. The correct references are as follows:

[1] D. Wade, *Chem.-Biol. Interact.* **1999**, *117*, 191–217 and [16] W. Wang, M. Pitoňák, P. Hobza, *ChemPhysChem* **2007**, *8*, 2107–2111. The authors apologize for the oversight.